Self-Assembly of Upright, Partially Dehydrogenated Melamine on Pd{111}

ARTICLE *in* THE JOURNAL OF PHYSICAL CHEMISTRY C · OCTOBER 2013

Impact Factor: 4.77 · DOI: 10.1021/jp407303e

3 AUTHORS:

John Greenwood
University of Leuven
10 PUBLICATIONS **48** CITATIONS
SEE PROFILE

Herbert A. Früchtl
University of St Andrews
44 PUBLICATIONS **524** CITATIONS
SEE PROFILE

Christopher J Baddeley
University of St Andrews
94 PUBLICATIONS **2,299** CITATIONS
SEE PROFILE

THE JOURNAL OF PHYSICAL CHEMISTRY C

Article

pubs.acs.org/JPCC

Self-Assembly of Upright, Partially Dehydrogenated Melamine on Pd(111)

John Greenwood, Herbert A. Früchtl, and Christopher J. Baddeley*

EaStCHEM School of Chemistry, University of St. Andrews, North Haugh, St. Andrews, Fife KY16 9ST, U.K.

ABSTRACT: The adsorption of melamine (1,3,5-triazine-2,4,6-triamine) on Pd(111) under ultrahigh-vacuum conditions was investigated using scanning tunneling microscopy and reflection−absorption infrared spectroscopy. At all coverages in the submonolayer regime, melamine was found to adsorb with its molecular plane perpendicular, or close to perpendicular, to the (111) surface. Following adsorption at 300 K, at low coverage, 1-D chains of partially dehydrogenated melamine are formed on the Pd surface aligned along the $\langle \overline{1}12 \rangle$ crystallographic directions. At higher coverage, pairing of melamine species is observed, and chain growth directions become less well-defined. The surface chemistry of melamine and the influence of the surface, coadsorbed hydrogen, and intermolecular interactions on the formation of ordered molecular arrangements are discussed.

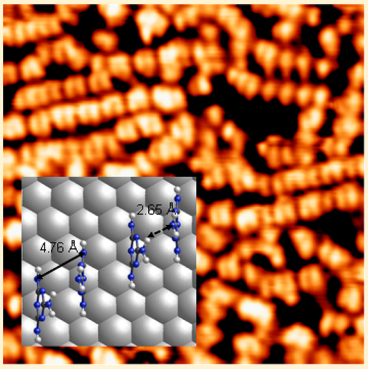

INTRODUCTION

The fabrication of 2-dimensional nanostructures utilizing organic molecular building blocks has been extensively researched. A variety of structures have been realized on a range of surfaces, utilizing noncovalent intermolecular forces, such as hydrogen bonds,[1−5] van der Waals forces,[6,7] and metal−organic coordination,[3,8,9] to produce ordered overlayer structures. There are advantages to utilizing hydrogen bonding for such structures, specifically that the relatively high equilibration rate of intermolecular interactions allows defects within supramolecular assemblies to be minimized, and high diffusion rates of small organic precursors coupled with the flexibility in hydrogen-bonding geometries enable extremely ordered structures to be created on a large scale.

Melamine (1,3,5-triazine-2,4,6-triamine, Figure 1a) is ubiquitous among hydrogen-bonded structures in the literature. The 3-fold rotational symmetry, and the multiple hydrogen-bonding interactions available between the hydrogen atoms of the amine groups and the triazine ring nitrogen atoms, make it a desirable molecular unit for nanoscale structures. So far, melamine adsorption has been investigated on the Au(111),[10] Ag(111),[11] Ni(111),[12] Cu(100),[13] and Cu(111)[14] surfaces. In addition, bimolecular hydrogen-bonded systems of melamine have been studied, incorporating cyanuric acid,[15,16] perylenetetracarboxylic dianhydride (PTCDA),[17] perylenetetracarboxylic diimide (PTCDI),[1,18,19] and naphthalenetetracarboxylic diimide (NTCDI).[20] Recently, a trimolecular system of melamine in combination with PTCDI and uracil has been investigated with scanning tunneling microscopy (STM).[21] Because of the low thermal stability of hydrogen-bonded structures, research has been conducted into developing surface confined covalent architectures, which possess higher thermal and mechanical stability. Covalently bonded two-dimensional nanostructures have been fabricated using melamine as the nucleophilic species, reacting with 1,4-phenylene diisocyanate[22] and with trimesoyl chloride,[23] both on Au(111), to produce urea and amide linkages, respectively. Melamine has also been combined with aromatic aldehydes under ambient conditions to produce oligomeric imine species.[24]

This study combines STM and reflection−absorption infrared spectroscopy (RAIRS) to examine the adsorption of melamine on Pd(111) in order to probe the possibility of using melamine (or other aromatic amines) as a building block for covalent architectures on palladium surfaces. Pd is a versatile metal for a range of catalytic transformations such as selective (and enantioselective) hydrogenation reactions,[25−27] and consequently, the ability to prepare functionalized polymer architectures on Pd has considerable potential in the development of novel Pd-based catalysts.

EXPERIMENTAL SECTION

The STM experiments were carried out on an Omicron ultrahigh-vacuum (UHV) system with a base pressure of 1×10^{-10} mbar. The Pd(111) sample was prepared by cycles of Ar ion bombardment (1.5 kV) and annealing to 893 K until a sharp (1×1) LEED pattern was observed, and STM indicated the presence of a clean Pd(111) surface. Melamine (Sigma-Aldrich, 99.9% purity) was deposited onto the Pd(111) surface, held at room temperature, from a glass doser resistively heated to 393 K, separated from the UHV chamber by a gate valve, and differentially pumped by a turbomolecular pump. STM images of the surface were acquired by transferring under UHV conditions to the STM chamber, where data were taken in constant current mode using an electrochemically etched W tip.

Received: July 23, 2013
Revised: September 24, 2013
Published: October 10, 2013

   dx.doi.org/10.1021/jp407303e | J. Phys. Chem. C 2013, 117, 22874−22879

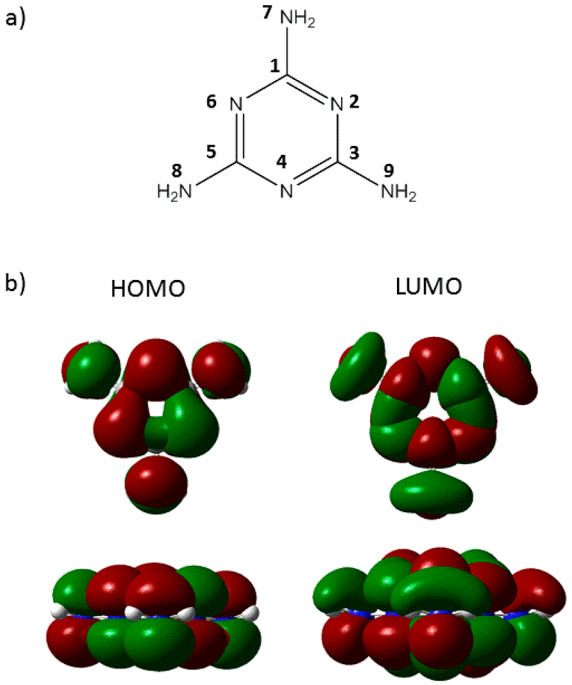

Figure 1. (a) Chemical structure of melamine with atom labels to aid explanation of vibrational assignments in Table 1. (b) HOMO and LUMO of melamine (Gaussian 03, density functional theory using the B3YLP functional with 6-31G* basis set), showing the front-on view to the left and top-down view to the right for the respective molecular orbitals.

All STM images were acquired at room temperature. STM images were processed using WSxM software.[28] RAIRS measurements were carried out in UHV using a Nicolet Nexus 860 FTIR spectrometer fitted with a mercury cadmium telluride (MCT) detector cooled by liquid nitrogen, possessing a spectral range of 800−4000 cm^{-1}. The spectrometer was operated with a resolution of 4 cm^{-1}, at 256 scans per spectrum.

DFT CALCULATIONS

Periodic DFT calculations were carried out using the VASP program,[29−31] using the PBE functional[32] a plane-wave basis set with an energy cutoff of 400 eV, PAW (projector augmented wave[33]) treatment of core electrons, and the VASP-supplied pseudopotentials for this method.[34] Binding energies of a doubly deprotonated melamine molecule were compared by optimizing the geometry of the molecule on a slab consisting of four layers of Pd, with a unit cell of 25 (5 × 5) atoms per layer. The uppermost Pd layer was allowed to relax during these optimizations, while the lower three were frozen at the optimized bulk geometry. Dipole correction[35] was applied to the direction orthogonal to the surface.

RESULTS

Reflection−Absorption Infrared Spectroscopy (RAIRS). The RAIR spectra shown in Figure 2 were acquired following the adsorption of melamine on Pd(111) at 300 K as a function of increasing exposure. At low melamine exposure, bands are observed at 1608, 1562, 1556 (appearing as a shoulder to the 1562 cm^{-1} band), 1475, and 1383 cm^{-1}. At higher coverage, an additional band is observed at 1392 cm^{-1}. As the melamine coverage is increased, there is a change in the relative intensity of the bands such that at the highest exposures the 1608 and 1392 cm^{-1} bands become relatively much more intense.

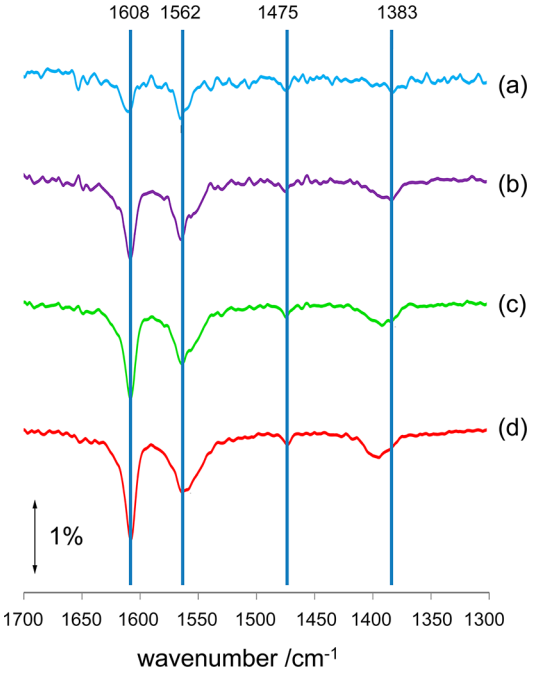

Figure 2. RAIR spectra as a function of increasing exposure following melamine adsorption on Pd (111) at 300 K. The cumulative melamine exposures are (a) 0.04, (b) 0.07, (c) 0.09, and (d) 0.11 langmuir.

Scanning Tunneling Microscopy (STM). Figure 3a shows an STM image of the Pd(111) surface following exposure to 0.04 langmuir of melamine at 300 K, approximately corresponding to the RAIR spectrum of Figure 2a. Under these conditions, chains of molecular features are observed along the three rotationally equivalent $\langle\bar{1}12\rangle$-type surface directions. A zoomed image of the low-coverage melamine chains is presented in Figure 3b. The individual melamine molecules within each chain are resolvable, separated by ∼6.5 Å. The distance of closest approach of melamine chains is measured to be ∼13 Å.

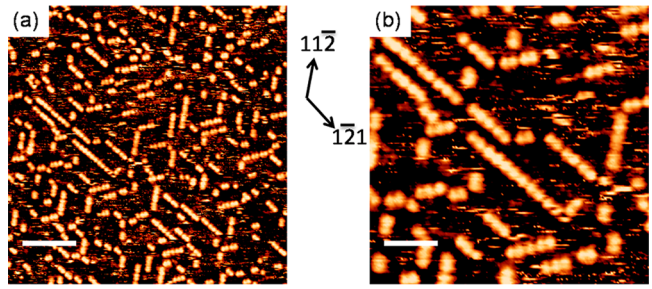

Figure 3. (a) STM image of melamine, ∼0.036 langmuir dose, adsorbed on Pd(111) at 300 K (scale bar 7.5 nm; 0.15 V, 0.3 nA). (b) A close-up image of the same surface (scale bar 3.2 nm).

Figure 4a shows an STM image of a melamine-covered Pd(111) surface after an exposure of 0.16 langmuir (i.e., corresponding to the high coverage melamine RAIR spectrum in Figure 2). There is no apparent long-range order in the melamine overlayer structure that is formed. One-dimensional chains are observed with growth directions similar to those

dx.doi.org/10.1021/jp407303e | J. Phys. Chem. C 2013, 117, 22874−22879

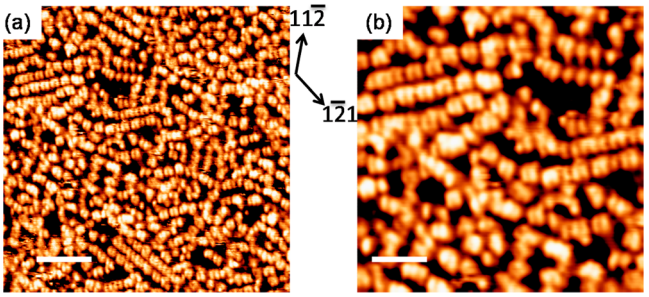

Figure 4. (a) STM image of melamine, ~0.16 langmuir, adsorbed on Pd(111) at 300 K (scale bar 6.6 nm; 1.5 V, 0.3 nA). (b) A close-up image of the same surface (scale bar 3.4 nm).

present at low coverage. However, the growth directions are no longer limited to the three rotationally equivalent ⟨$\bar{1}$12⟩-type directions. In many of the chains, molecular features appear to pair up such that the average spacing between molecules is ~6.2 Å, but the spacings alternate from ~5.2 to ~7.2 Å.

DISCUSSION

RAIRS. Table 1 summarizes the vibrational band assignments for melamine on Pd(111) and provides a comparison of

Table 1. Vibrational Frequencies and Assignments for Melamine on Pd(111)[a]

melamine/ Pd(111) υ (cm^{-1})	melamine/ Ni(111)[12] υ (cm^{-1})	melamine/gas-phase[36] υ (cm^{-1})	vibrational mode assignments
		3571 m	υ NH_2^{asym}
	3442 w	3453 m	υ NH_2^{sym}
1608 vs	1612 vs	1598 vs	β NH_2^{sym}, υ $C_{(1)}N_{(7)}$, aromatic ring breathing
	1593 s		β NH_2^{sym}, $(\upsilon C_{(5)}N_{(6)}, \upsilon C_{(3)}N_{(2)})^{sym}$
1562 s, 1556 m	1560 m	1556 m	$\upsilon C_{(1)}N_{(2)}$, $\upsilon C_{(5)}N_{(4)}$
1475 m	1477 m	1440 s	ring breathing, $\upsilon N_{(7)}C_{(1)}$
	1458 w		in-plane aromatic ring stretch
1392 s, 1383 m	1402 s		$(\upsilon C_{(5)}N_{(6)}, \upsilon C_{(3)}N_{(2)})^{asym}$
	1240 w		$\beta N_{(8)}H$, $\beta N_{(9)}H$

[a]Notation of symbols used: υ = stretch, β = bend. Abbreviations: vs = very strong, s = strong, m = medium, w = weak, sym = symmetrical, asym = asymmetrical. The vibrational mode assignments are taken from ref 12.

the observed bands with those from melamine/Ni(111) and gas phase melamine. There is a strong correspondence between the RAIR spectra of melamine on Pd(111) with the gas phase spectrum[36] and those reported for melamine on Ni(111).[12] In our work on the melamine/Ni(111) system, we concluded that two of the amine functionalities of melamine underwent partial or full dehydrogenation to enable a strong metal−molecule interaction via the two dehydrogenated N atoms and one N atom of the triazine ring. DFT calculations predicted an adsorption geometry whereby the plane of the aromatic ring was perpendicular to the Ni(111) surface.[12]

In contrast to the melamine/Ni(111) system,[12] there is no strong coverage dependence to the melamine/Pd(111) RAIR spectra. At high submonolayer coverage, the melamine/Pd(111) spectrum is dominated by intense bands at 1606 and 1562 cm^{-1}. The peak observed at 1606 cm^{-1} lies between the 1593 and 1612 cm^{-1} bands observed on Ni(111) whose relative intensities are strongly coverage dependent. Each of these bands can be assigned to the NH_2 scissor mode.[12] There are also three weaker peaks observed at 1551, 1471, and 1394 cm^{-1} for saturation coverage, which also correlate closely to observed peaks for the Ni system at 1560, 1477, and 1402 cm^{-1}, respectively.

The presence of relatively intense bands in the melamine/Pd(111) system indicates, by application of the metal−surface dipole selection rule, that the plane of the aromatic ring of melamine is not parallel to the (111) surface plane. This contrasts to the behavior of melamine on Au(111)[37] and Ag(111)[11] where a flat-lying geometry is adopted with the molecular layer being stabilized by strong intermolecular H-bonding interactions. A geometry with the molecular plane perpendicular to the surface has also been reported for melamine on copper single crystal surfaces.[13,14] The high resolution electron energy loss spectra (HREELS) of pyridine adsorbed on Pt(111) at 310 K[38] provide a useful comparison to that of the vibrational spectra of melamine on Pd(111). Loss peaks, among others, were observed in the specular direction at 1340 (w), 1460 (m), and 1570 cm^{-1} (vw); these were assigned as C−C ring stretch, C−C, C−N stretch, and C−C, C−N stretch, respectively; these values are in good agreement with the IR peaks observed in the present study at 1392 (s), 1475 (m), and 1562 cm^{-1} (s), respectively. The authors proposed that pyridine behaves as a Lewis acid, donating electron density through the nitrogen electron lone pair into the Pd surface. These results are in agreement with a study by Netzer and Mack[39] of pyridine on Pd(111) using ultraviolet photoelectron spectroscopy (UPS) and HREELS. Pyridine adsorption at 300 K has been shown by HREELS[38] and RAIRS[40] to form an α-pyridyl species in an upright configuration when adsorbed on Pt(111), independent of coverage. Grassian and Muetterties studied the vibrational spectra of pyridine adsorption on Pd(111) using HREELS.[41] The results showed that at 310 K, and at saturation coverage, pyridine is chemisorbed to the surface with the plane of the aromatic ring oriented away from the surface plane. The similarity between the vibrational frequencies of adsorbed pyridine and melamine is consistent with an upright adsorption mode for melamine on Pd(111).

STM. Further support for the conclusions regarding adsorption orientation come from the shape of the features observed in STM; DFT calculations were carried out (Gaussian 03, 6-31G*, B3LYP) of the highest occupied molecular orbital (HOMO) and lowest occupied molecular orbital (LUMO) for isolated melamine. Figure 1a shows the chemical structure of melamine; the numerical labels adjacent to the carbon and nitrogen atoms are referred to in Table 1 in order to aid the assignment of the molecular vibrations. Figure 1b shows each orbital viewed perpendicular and parallel to the plane of the aromatic ring. Though adsorption of melamine on Pd(111) will undoubtedly alter the appearance of the HOMO and LUMO via coupling with the Pd d band, the orbital appearance should still be comparable to the shape of the adsorbed molecules in the STM images. Under the imaging conditions used (i.e., tip biased negatively), one would anticipate that the imaged molecule may resemble the LUMO in appearance, with electrons being transferred from filled tip states to empty sample states. The cylindrical features observed in STM are consistent with the LUMO viewed parallel to the aromatic ring,

dx.doi.org/10.1021/jp407303e | J. Phys. Chem. C 2013, 117, 22874−22879

implying that melamine adsorbs with the aromatic ring either perpendicular to the surface or at least strongly tilted with respect to the surface. On Au, where melamine is known to adsorb with the molecular plane parallel to the surface,[37] the molecular features appear triangular in STM consistent with the view of the LUMO from perpendicular to the aromatic ring.

Strong similarities exist between the STM images of melamine on Pd(111) and those previously observed on Ni(111).[12] In each case, molecular features are observed to grow in chains along the $\langle 1\bar{1}2\rangle$ type directions of the metal surface. On Ni, molecular chains were found to have very well-defined growth directions.[12] In contrast, on Pd, the melamine chains have a greater tendency to curve (Figure 4). In addition, on Pd, the melamine features along chains are often observed to pair up to give alternating intermolecular spacings. On Ni, the partially dehydrogenated melamine is able to adopt a stable bridge-atop-bridge adsorption geometry due to the matching of the molecular and substrate dimensions.[12] Our DFT calculations found that such an adsorption geometry is also the lowest energy configuration on Pd(111). We believe that the differences between the packing behavior of melamine on Ni and Pd are likely to be at least partly associated with the ∼10% lattice mismatch between the two metals coupled with the slight difference in reactivity of the two metals. On Ni(111), a strong tendency to order with an intermolecular spacing of 4.3 Å is observed. On Pd, the spacing between equivalent bridge-atop-bridge sites along the $\langle 1\bar{1}2\rangle$ direction is 4.76 Å. A larger intermolecular spacing would be expected to lead to a decrease in intermolecular repulsion. However, on Pd, molecules are not found to form extended straight rows with this intermolecular separation. Instead, in most chains, molecular spacings are found to alternate between ∼5 and ∼7 Å. This separation is consistent with the model presented in Figure 5b where pairs of melamine species propagate along $\langle \bar{3}25\rangle$-type directions giving a pair repeat distance of 12.0 Å. The net effect is that the chain is no longer oriented directly along the $\langle 1\bar{1}2\rangle$ direction but propagates along a lower symmetry direction. Three rotationally equivalent growth directions would exist, and in the absence of any chiral influence, there would be a mirror equivalent growth direction for each chain structure. DFT provides an explanation for these observations as shown in Figure 5a. The "pairing" of melamine molecules was investigated using a "sparse" chain, following the $\langle \bar{3}25\rangle$ direction that seems most consistent with STM observation, as well as a "dense" chain along the $\langle 1\bar{1}2\rangle$ direction (as shown in Figure 5a). In each case, the bases of each molecule are separated by the $\sqrt{3}$ distance (4.76 Å on the real Pd surface; 4.83 Å based on a bulk optimization in the DFT calculation). During these pair calculations, an empirical VdW correction[42] was applied. In each case, placing an array of melamine molecules in bridge-atop-bridge adsorption sites along a $\langle 1\bar{1}2\rangle$ direction and optimizing the structure results in pairs of adjacent melamine species leaning toward each other. The driving force for this slight tilting of the molecular planes appears to be the ability to produce a hydrogen bond of distance 2.65 Å between adjacent NH_2 groups. It is not clear from the DFT calculations why the pairs of molecules do not align in extended rows along the $\langle 1\bar{1}2\rangle$ directions. No energetic preference was found for the "sparse" arrangements over the "dense" arrangements. On Ni, though the intermolecular separation is smaller, molecules are presumably able to align along the $\langle 1\bar{1}2\rangle$ direction since the adsorption energy of a given melamine species is significantly stronger than on Pd. Not only

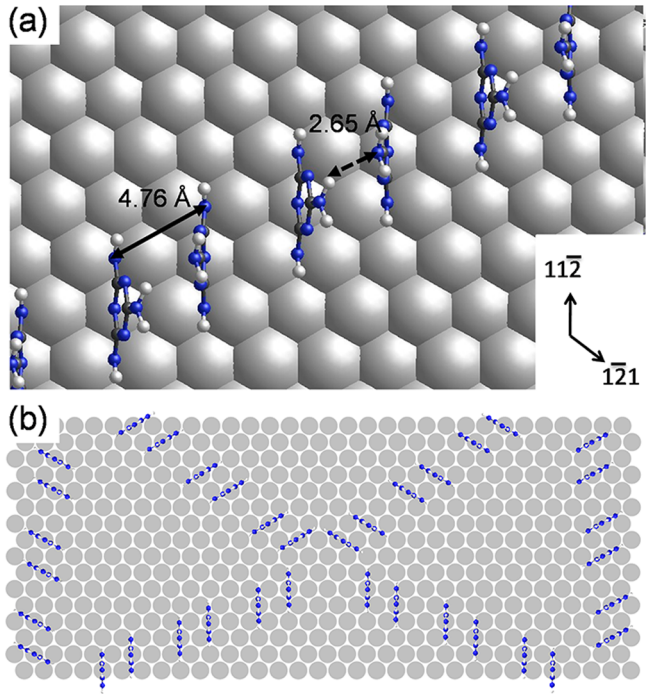

Figure 5. (a) Diagram showing the outcome of a DFT calculation on the structure of partially dehydrogenated melamine species arranged along a $\langle 1\bar{1}2\rangle$-type surface direction of a Pd(111) slab. Melamine species are observed to pair up driven by the formation of an intermolecular hydrogen bond. (b) Schematic diagram showing the possible origin of the chains of paired melamine features observed in the STM images.

do molecules generally adsorb more strongly on Ni than on Pd, but in order for melamine to adopt the bridge-atop-bridge site on Pd, the intramolecular bonding is considerably more distorted than on Ni. Hence, the strongly favorable adsorption energy overcomes lateral repulsions on Ni. The subtle difference in the RAIR spectra at high coverage on Ni(111)[12] and Pd(111) can be explained by the differences in intermolecular spacing on the two surfaces. On Ni, at high coverage, two bands are observed at 1593 and 1612 cm^{-1},[12] whereas on Pd, a single peak is observed at all coverages in this frequency range. On Ni, the 1612 cm^{-1} band increases in relative intensity with increasing coverage and was associated with densely packed melamine species.[12] The greater intermolecular spacing observed in STM for melamine on Pd(111) may be insufficient to induce the splitting of these IR bands.

Undoubtedly, on both Ni[43,44] and Pd[44] surfaces, hydrogen atoms released by the dehydrogenation of melamine will be stable at 300 K. The structures resulting from supramolecular growth of terephthalic acid on Pd(111)[45] were shown to be dynamically controlled by a self-limiting deprotonation process. The population of surface sites with hydrogen atoms reduces the reactivity of the surface and prevents subsequent dissociative adsorption. In both the Pd and Ni cases, it is likely that the presence of coadsorbed hydrogen has a similar effect limiting the formation of high density structures of partially dehydrogenated melamine. The density of chains observed on Pd is significantly lower than on Ni,[12] implying that the influence of coadsorbed hydrogen is stronger on Pd. Future experiments employing deliberate codosing of H_2 or

dx.doi.org/10.1021/jp407303e | J. Phys. Chem. C 2013, 117, 22874−22879

adsorption at elevated temperatures could prove instructive in understanding this behavior.

The presence of an $-NH_2$ group pointing away from the surface containing a reactive nitrogen electron lone pair holds potential for reaction and the growth of surface architectures in three dimensions. For example, Buck and co-workers[46] have demonstrated the deposition of Pd nanoparticles on pyridine terminated self-assembled monolayers on Au/mica in ambient conditions. Alternatively, melamine can be used within SAMs to modify the structures as has been demonstrated previously with Cu deposition on SAMs.[18] It would be interesting to investigate whether the strong interaction between melamine and Pd can be utilized to anchor Pd nanoparticles to SAMs.

CONCLUSIONS

RAIRS data following melamine adsorption on Pd(111) at 300 K give intense bands for in-plane vibrational modes of melamine, suggesting an adsorption geometry whereby the plane of the aromatic ring is tilted with respect to the surface plane at all coverages in the submonolayer regime. There is no significant coverage dependent shift in vibrational bands with coverage.

At low coverage, STM reveals the formation of one-dimensional filament structures aligned predominantly along $\langle\overline{1}12\rangle$-type surface directions. At higher coverage, the 1-D structures have a tendency to curve. Along a given chain of molecules, a strong tendency is observed for the molecules to pair up such that there is an alternation of intermolecular spacings. DFT calculations suggest that the driving force for the pairing of molecules is the possibility to form a hydrogen-bonding interaction between NH_2 groups on adjacent molecules. Melamine is adsorbed via σ-donation to the surface from a triazine nitrogen atom and two adjacent amino group nitrogen atoms which are probably partially or fully dehydrogenated by analogy with the behavior of melamine on Ni(111).[12] The subtle differences in behavior between melamine on Pd(111) compared to Ni(111) is ascribed to the 10% difference in lattice mismatch which will influence the adsorption site of melamine coupled with the difference in reactivity between the two surfaces and the likelihood that coadsorbed hydrogen influences the supramolecular assembly of melamine species.

AUTHOR INFORMATION

Corresponding Author

*E-mail cjb14@st-and.ac.uk; tel +44 1334 467236 (C.J.B.).

Notes

The authors declare no competing financial interest.

ACKNOWLEDGMENTS

We are grateful to Prof. Neville Richardson for access to his RAIRS and STM instruments. J.G. acknowledges EPSRC for funding his Ph.D studentship. Computational support was provided via the EaStCHEM research computing facility.

REFERENCES

(1) Theobald, J. A.; Oxtoby, N. S.; Phillips, M. A.; Champness, N. R.; Beton, P. H. Controlling Molecular Deposition and Layer Structure with Supramolecular Surface Assemblies. *Nature* **2003**, *424*, 1029–1031.

(2) Kudernac, T.; Lei, S. B.; Elemans, J.; De Feyter, S. Two-Dimensional Supramolecular Self-Assembly: Nanoporous Networks on Surfaces. *Chem. Soc. Rev.* **2009**, *38*, 3505–3505.

(3) Barth, J. V. Molecular Architectonic on Metal Surfaces. *Annu. Rev. Phys. Chem.* **2007**, *58*, 375–407.

(4) De Feyter, S.; De Schryver, F. C. Self-Assembly at the Liquid/Solid Interface: Stm Reveals. *J. Phys. Chem. B* **2005**, *109*, 4290–4302.

(5) De Feyter, S.; Miura, A.; Yao, S.; Chen, Z.; Wurthner, F.; Jonkheijm, P.; Schenning, A.; Meijer, E. W.; De Schryver, F. C. Two-Dimensional Self-Assembly into Multicomponent Hydrogen-Bonded Nanostructures. *Nano Lett.* **2005**, *5*, 77–81.

(6) Furukawa, S.; Tahara, K.; De Schryver, F. C.; Van der Auweraer, M.; Tobe, Y.; De Feyter, S. Structural Transformation of a Two-Dimensional Molecular Network in Response to Selective Guest Inclusion. *Angew. Chem., Int. Ed.* **2007**, *46*, 2831–2834.

(7) Blum, M. C.; Cavar, E.; Pivetta, M.; Patthey, F.; Schneider, W. D. Conservation of Chirality in a Hierarchical Supramolecular Self-Assembled Structure with Pentagonal Symmetry. *Angew. Chem., Int. Ed.* **2005**, *44*, 5334–5337.

(8) Stepanow, S.; Lingenfelder, M.; Dmitriev, A.; Spillmann, H.; Delvigne, E.; Lin, N.; Deng, X. B.; Cai, C. Z.; Barth, J. V.; Kern, K. Steering Molecular Organization and Host-Guest Interactions Using Two-Dimensional Nanoporous Coordination Systems. *Nat. Mater.* **2004**, *3*, 229–233.

(9) Lin, N.; Stepanow, S.; Ruben, M.; Barth, J. V. In *Templates in Chemistry III*; Springer-Verlag: Berlin, 2009; Vol. *287*, pp 1–44.

(10) Silly, F.; Shaw, A. Q.; Castell, M. R.; Briggs, G. A. D.; Mura, M.; Martsinovich, N.; Kantorovich, L. Melamine Structures on the Au(111) Surface. *J. Phys. Chem. C* **2008**, *112*, 11476–11480.

(11) Schmitz, C. H.; Ikonomov, J.; Sokolowski, M. Two Commensurate Hydrogen-Bonded Monolayer Structures of Melamine on Ag(111). *Surf. Sci.* **2011**, *605*, 1–6.

(12) Greenwood, J.; Früchtl, H. A.; Baddeley, C. J. Ordered Growth of Upright Melamine Species on Ni{111}: A Study with Scanning Tunnelling Microscopy and Reflection Absorption Infrared Spectroscopy. *J. Phys. Chem. C* **2012**, *116*, 6685–6690.

(13) Pan, S.; Fu, Q.; Huang, T.; Zhao, A.; Wang, B.; Luo, Y.; Yang, J.; Hou, J. Design and Control of Electron Transport Properties of Single Molecules. *Proc. Natl. Acad. Sci. U. S. A.* **2009**, *106*, 15259–15263.

(14) Lin, Y.-P.; Ourdjini, O.; Giovanelli, L.; Clair, S.; Faury, T.; Ksari, Y.; Themlin, J.-M.; Porte, L.; Abel, M. Self-Assembled Melamine Monolayer on Cu(111). *J. Phys. Chem. C* **2013**, *117*, 9895–9902.

(15) Zhang, H. M.; Xie, Z. X.; Long, L. S.; Zhong, H. P.; Zhao, W.; Mao, B. W.; Xu, X.; Zheng, L. S. One-Step Preparation of Large-Scale Self-Assembled Monolayers of Cyanuric Acid and Melamine Supramolecular Species on Au(111) Surfaces. *J. Phys. Chem. C* **2008**, *112*, 4209–4218.

(16) Zhang, H. M.; Pei, Z. K.; Xie, Z. X.; Long, L. S.; Mao, B. W.; Xu, X.; Zheng, L. S. Preparing Self-Assembled Monolayers of Cyanuric Acid and Melamine Complex on Hopg Surfaces. *J. Phys. Chem. C* **2009**, *113*, 13940–13946.

(17) Swarbrick, J. C.; Rogers, B. L.; Champness, N. R.; Beton, P. H. Hydrogen-Bonded Ptcda-Melamine Networks and Mixed Phases. *J. Phys. Chem. B* **2006**, *110*, 6110–6114.

(18) Madueno, R.; Raisanen, M. T.; Silien, C.; Buck, M. Functionalizing Hydrogen-Bonded Surface Networks with Self-Assembled Monolayers. *Nature* **2008**, *454*, 618–621.

(19) Perdigao, L. M. A.; Perkins, E. W.; Ma, J.; Staniec, P. A.; Rogers, B. L.; Champness, N. R.; Beton, P. H. Bimolecular Networks and Supramolecular Traps on Au(111). *J. Phys. Chem. B* **2006**, *110*, 12539–12542.

(20) Keeling, D. L.; Oxtoby, N. S.; Wilson, C.; Humphry, M. J.; Champness, N. R.; Beton, P. H. Assembly and Processing of Hydrogen Bond Induced Supramolecular Nanostructures. *Nano Lett.* **2003**, *3*, 9–12.

(21) Gardener, J. A.; Shvarova, O. Y.; Briggs, G. A. D.; Castell, M. R. Intricate Hydrogen-Bonded Networks: Binary and Ternary Combinations of Uracil, Ptcdi, and Melamine. *J. Phys. Chem. C* **2010**, *114*, 5859–5866.

(22) Jensen, S.; Früchtl, H. A.; Baddeley, C. J. Coupling of Triamines with Diisocyanates on Au(111) Leads to the Formation of Polyurea Networks. *J. Am. Chem. Soc.* **2009**, *131*, 16706–16713.

(23) Jensen, S.; Greenwood, J.; Früchtl, H. A.; Baddeley, C. J. STM Investigation on the Formation of Oligoamides on Au{111} by Surface-Confined Reactions of Melamine with Trimesoyl Chloride. *J. Phys. Chem. C* **2011**, *115*, 8630−8636.
(24) Greenwood, J.; Baddeley, C. J. Formation of Imine Oligomers on Au under Ambient Conditions Investigated by Scanning Tunneling Microscopy. *Langmuir* **2012**, *29*, 653−657.
(25) Studer, M.; Blaser, H. U.; Exner, C. Enantioselective Hydrogenation Using Heterogeneous Modified Catalysts: An Update. *Adv. Synth. Catal.* **2003**, *345*, 45−65.
(26) Huck, W. R.; Mallat, T.; Baiker, A. Coadsorption of Cinchona Alkaloids on Supported Palladium: Nonlinear Effects in Asymmetric Hydrogenation and Resistance of Alkaloids against Hydrogenation. *Catal. Lett.* **2003**, *87*, 241−247.
(27) Huck, W. R.; Burgi, T.; Mallat, T.; Baiker, A. Palladium-Catalyzed Enantio Selective Hydrogenation of 2-Pyrones: Evidence for Competing Reaction Mechanisms. *J. Catal.* **2003**, *219*, 41−51.
(28) Horcas, I.; Fernandez, R.; Gomez-Rodriguez, J. M.; Colchero, J.; Gomez-Herrero, J.; Baro, A. M. Wsxm: A Software for Scanning Probe Microscopy and a Tool for Nanotechnology. *Rev. Sci. Instrum.* **2007**, *78*.
(29) Kresse, G.; Hafner, J. Ab Initio Molecular-Dynamics for Liquid-Metals. *Phys. Rev. B* **1993**, *47*, 558−561.
(30) Kresse, G.; Furthmüller, J. Efficient Iterative Schemes for Ab Initio Total-Energy Calculations Using a Plane-Wave Basis Set. *Phys. Rev. B* **1996**, *54*, 11169−11186.
(31) Kresse, G.; Furthmüller, J. Efficiency of Ab-Initio Total Energy Calculations for Metals and Semiconductors Using a Plane-Wave Basis Set. *Comput. Mater. Sci.* **1996**, *6*, 15−50.
(32) Perdew, J. P.; Burke, K.; Ernzerhof, M. Generalized Gradient Approximation Made Simple. *Phys. Rev. Lett.* **1996**, *77*, 3865−3868.
(33) Blöchl, P. E. Projector Augmented-Wave Method. *Phys. Rev. B* **1994**, *50*, 17953−17979.
(34) Kresse, G.; Joubert, D. From Ultrasoft Pseudopotentials to the Projector Augmented-Wave Method. *Phys. Rev. B* **1999**, *59*, 1758−1775.
(35) Neugebauer, J.; Scheffler, M. Adsorbate-Substrate and Adsorbate-Adsorbate Interactions of Na and K Adlayers on Al(111). *Phys. Rev. B* **1992**, *46*, 16067−16080.
(36) Wang, Y. L.; Mebel, A. M.; Wu, C. J.; Chen, Y. T.; Lin, C. E.; Jiang, J. C. IR Spectroscopy and Theoretical Vibrational Calculation of the Melamine Molecule. *J. Chem. Soc., Faraday Trans.* **1997**, *93*, 3445−3451.
(37) Silly, F.; Shaw, A. Q.; Castell, M. R.; Briggs, G. A. D.; Mura, M.; Martsinovich, N.; Kantorovich, L. Melamine Structures on the Au(111) Surface. *J. Phys. Chem. C* **2008**, *112*, 11476−11480.
(38) Grassian, V. H.; Muetterties, E. L. Electron Energy Loss and Thermal Desorption Spectroscopy of Pyridine Adsorbed on Platinum(111). *J. Phys. Chem.* **1986**, *90*, 5900−5907.
(39) Netzer, F. P.; Mack, J. U. The Electronic Structure of Aromatic Molecules Adsorbed on Pd(111). *J. Chem. Phys.* **1983**, *79*, 1017−1025.
(40) Haq, S.; King, D. A. Configurational Transitions of Benzene and Pyridine Adsorbed on Pt{111} and Cu{110} Surfaces: An Infrared Study. *J. Phys. Chem.* **1996**, *100*, 16957−16965.
(41) Grassian, V. H.; Muetterties, E. L. Vibrational Electron Energy Loss Spectroscopic Study of Benzene, Toluene, and Pyridine Adsorbed on Palladium(111) at 180 K. *J. Phys. Chem.* **1987**, *91*, 389−396.
(42) Grimme, S. Semiempirical Gga-Type Density Functional Constructed with a Long-Range Dispersion Correction. *J. Comput. Chem.* **2006**, *27*, 1787−1799.
(43) Russell, J. J. N.; Gates, S. M.; Yates, J. J. T. Isotope Effects in Hydrogen Adsorption on Ni(111): Direct Observation of a Molecular Precursor State. *J. Chem. Phys.* **1986**, *85*, 6792−6802.
(44) Eberhardt, W.; Louie, S. G.; Plummer, E. W. Interaction of Hydrogen with a Pd(111) Surface. *Phys. Rev. B* **1983**, *28*, 465−477.
(45) Canas-Ventura, M. E.; Klappenberger, F.; Clair, S.; Pons, S.; Kern, K.; Brune, H.; Strunskus, T.; Woll, C.; Fasel, R.; Barth, J. V. Coexistence of One- and Two-Dimensional Supramolecular Assemblies of Terephthalic Acid on Pd(111) Due to Self-Limiting Deprotonation. *J. Chem. Phys.* **2006**, *125*.
(46) Silien, C.; Lahaye, D.; Caffio, M.; Schaub, R.; Champness, N. R.; Buck, M. Electrodeposition of Palladium onto a Pyridine-Terminated Self-Assembled Monolayer. *Langmuir* **2011**, *27*, 2567−2574.